

# Rho-associated kinase1 promotes Laryngeal squamous cell carcinoma tumorigenesis and progression via the FAK pathway

Li-Yun YANG

Peipei Qiao

Jianwei Zhang

An Hu ([✉ juanitohuan@163.com](mailto:juanitohuan@163.com))

---

## Research Article

**Keywords:** LSCC, ROCK1, tumorigenesis and progression, FAK

**Posted Date:** May 10th, 2022

**DOI:** <https://doi.org/10.21203/rs.3.rs-1630226/v1>

**License:**  This work is licensed under a Creative Commons Attribution 4.0 International License.

[Read Full License](#)

---

## Abstract

Laryngeal squamous cell carcinoma (LSCC) is one of the most common head and neck cancers. Rho-associated kinase1 (ROCK1) is believed to promote progression of most cancers, however, its role of LSCC is still unknown at present. In the study, ROCK1 is highly expressed in human LSCC tissues, and high expression of ROCK1 correlates with advanced stage and poor survival prognosis for LSCC patients. Decreasing ROCK1 expression inhibits the ability of progression, migration, invasion in vitro, as well as pulmonary metastasis in vivo, on the contrary, increasing ROCK1 expression has the opposite experimental results. FAK signalling pathway plays an essential role in promoting LSCC progression and inhibits FAK activity with TAE226, a specific FAK inhibitor, observably impairs the tumor-promoting effects induced by ROCK1. In conclusion, ROCK1 promotes LSCC tumorigenesis and progression via the FAK pathway, targeting ROCK1/FAK might provide a potential treatment strategy for LSCC.

## Introduction

Laryngeal squamous cell carcinoma (LSCC) is one of the most common head and neck cancers [1]. We have witnessed a continuing progress in LSCC treatment, nonetheless the 5-year survival rate of LSCC patients is only 68% [2]. Therefore, clarifying the mechanism of tumorigenesis and progression is of great significance for developing effective clinical prevention programs and new targeted therapies for LSCC.

Rho-associated kinase1 (ROCK1) is a classic serine/threonine protein kinase. ROCK1 carboxyl terminal structure can inhibit the amino-terminal kinase domain. ROCK1 can regulates downstream substrates such as muscle Globulin, adducin and protein kinases [3]. ROCKs function as versatile kinases, phosphorylating various substrates such as myosin light chain (MLC) phosphatase, LIM kinase, PTEN, insulin receptor substrate (IRS), ezrin/radixin/moesin (ERM) proteins, and JNK interacting protein (JIP-3) [4–6]. Recently, accumulating evidences have indicated that ROCK1 plays a crucial role in tumorigenesis and progression. Overexpression or activation of ROCK1 induces proliferation, while inhibition of ROCK1 by interfering RNA or inhibitors markedly decreased migration [7]. Stadler et al. also found that CAFs in the tumor microenvironment could promote colorectal cancer metastasis via targeting ROCK1 [8]. Although ROCK1 makes a contribution to tumor progression and metastasis, the specific molecular mechanism is unknown.

In the present study, we exhibit ROCK1 is highly expressed in human LSCC tissues compared to normal tissues, and high expression of ROCK1 correlates with advanced stage and poor survival prognosis for LSCC patients. Decreasing ROCK1 expression via siRNA inhibits the ability of progression, migration and invasion in vitro, as well as pulmonary metastasis in vivo, on the contrary, increasing ROCK1 expression via plasmid transfection has the opposite experimental results. FAK signalling pathway plays an essential role in promoting LSCC progression and inhibit FAK activity with TAE226, a specific FAK inhibitor, observably impairs the tumor-promoting effects induced by ROCK1. Those findings indicate that ROCK1 promotes LSCC tumorigenesis and progression via the FAK pathway, targeting ROCK1/FAK might provide a potential treatment strategy for LSCC.

# Results

## 1. ROCK1 is highly expressed in LSCC and related to poor survival

To demonstrate the role of ROCK1 in LSCC, qRT-PCR was applied to assess the expression level of ROCK1 in 30 LSCC. Results exhibited that ROCK1 mRNA level was dramatically higher in tumor tissues than matched adjacent non-tumor tissues (\*\*P < 0.01, Fig. 1A). In addition, ROCK1 overexpression was assessed in using immunohistochemistry (IHC). 24 of 30 LSCC tissues (the positive rate: 80%) were categorized as ROCK1 protein expression positive, whereas 6 LSCC tissues and 30 adjacent normal tissues (the positive rate of adjacent normal tissues: 47%) were categorized as ROCK1 protein negative or weak expression. Moreover, results of qRT-PCR and Western Blot were showed that the expression of ROCK1 was higher in Hep2, NH8, TU686 and TU212 cells (Fig. 1C-1D). Furthermore, the relationship between ROCK1 and clinicopathological features of 60 LSCC patients was showed in Table 1. ROCK1 high expression level in LSCC was markedly related to invasion range (P = 0.028), lymph node involvement (P = 0.019) and TNM stage (P < 0.001). But ROCK1 expression was not related to other clinicopathological characteristics such as age (P = 0.122), tumor size (P = 0.232) or gender (P = 0.521). Furthermore, 60 LSCC patients were followed up by 5 years, which 28 patients had died. The mortality was 46.7% (28 of 60, Fig. 1E, P = 0.0067). Above observations indicated that ROCK1 is highly expressed in LSCC and related to poor survival.

**Table 1. Relationship between ROCK1 expression level and clinicopathological characteristics in 60 LSCC patients.**

clinicopathological characteristics	ROCK1 staining		P
	Weak	Strong	
Age(years)			
≤60	14	16	0.122
≥60	11	19	
Gender			
Male	20	16	0.521
Female	18	6	
tumor size (cm)			
≤5	19	18	0.232
≥5	20	13	
invasion range			
T1, T2	13	11	0.028
T3, T4	20	16	
lymph node involvement			
No	9	14	0.019
Yes	24	15	
TNM stage			
I+II	8	16	0.001
III+IV	25	11	

## 2. ROCK1 promotes LSCC cells growth

Considering that ROCK1 is closely related to the occurrence and development of LSCC, we hypothesized whether the regulation of ROCK1 expression affect LSCC cells growth. ROCK1-siRNA was transfected to silence the expression of ROCK1 and plasmid (ROCK1, Myc-ROCK1-Delta3 (1-727), p-CAG-Myc) was transfected to increase the expression of ROCK1. The effect knockdown and upregulation were very obvious. Results of Immunofluorescent (IF) and Western Blot displayed that the expression of ROCK1 was obviously cut down in TU686 (TU686/si-ROCK1) and TU212 cells (TU212/si-ROCK1) in comparison with negative controls (TU686/si-nc, TU212/si-nc, Fig. 2A-B). The expression of ROCK1 was markedly enhanced in TU686/ROCK1 and TU212/ROCK1 cells in comparison with negative controls (TU686/vector, TU212/vector, Fig. 2C-D). Distinctly, knockdown of ROCK1 showed reduced cell proliferation (\*P < 0.05, Fig. 2E-F). While, TU686/ROCK1 and TU212/ROCK1 cells proliferated faster than TU686/vector and TU212/vector cells (\*\*P < 0.05, Fig. 2G-H). Moreover, results of flow cytometry showed that the percentage

of apoptotic cells was significantly higher in TU686/si-ROCK1 ( $22 \pm 2.45$ ) and TU212/si-ROCK1 cells ( $54 \pm 7.42$ ) than in TU686/si-nc ( $4 \pm 1.41$ ) and TU212/si-nc cells ( $10 \pm 2.44$ , \*\* $P < 0.01$ , Fig. 2I-J). A colony formation assay was used to further verify the proliferative effect of ROCK1 and the results exhibited the number of colonies from TU686/ROCK1 and TU212/ROCK1 cells was more than TU686/vector and TU212/vector cells (\*\* $P < 0.01$ , Fig. 2K-L). Together, above observations suggests ROCK1 promotes LSCC cells growth.

### 3. ROCK1 promotes LSCC cells migration and invasion

Transwell assays were performed to further identify the role of ROCK1 on the tumorigenesis and progression of LSCC. Results indicated more TU686/si-nc ( $74 \pm 9.17$ ) and TU212/si-nc cells ( $89 \pm 4.36$ ) migrated through transwell chambers compared with TU686/si-ROCK1 ( $37 \pm 7.0$ ) and TU212/si-ROCK1 cells ( $41 \pm 3.51$ ). Finally, invasion assays showed that TU686/si-nc ( $32 \pm 5.03$ ) and TU212/si-nc cells ( $39 \pm 2.31$ ) moved through matrigel more frequently than TU686/si-ROCK1 ( $13 \pm 1.52$ ) and TU212/si-ROCK1 cells ( $18 \pm 3.51$ , \*\* $P < 0.01$ , Fig. 3A-C). Inversely, less TU686/vector ( $45 \pm 7.51$ ) and TU212/vector cells ( $31 \pm 3.79$ ) migrated through transwell chambers compared with TU686/ROCK1 ( $95 \pm 7.21$ ) and TU212/ROCK1 cells ( $63 \pm 9.07$ ). And invasion assays showed that TU686/vector ( $19 \pm 5.00$ ) and TU212/vector cells ( $17 \pm 4.04$ ) moved through matrigel less frequently than TU686/ROCK1 ( $41 \pm 4.04$ ) and TU212/ROCK1 cells ( $32 \pm 2.52$ , \*\* $P < 0.01$ , Fig. 3D-F). Above results implies ROCK1 promotes LSCC cells migration and invasion.

### 4. The tumor-promoting effects induced by ROCK1 in LSCC are mediated through the activation of FAK signalling pathway

The FAK signalling pathway plays a crucial role in the migration and invasion of cancers [9–13]. We suggested that ROCK1 might mediate FAK signalling pathway to the migration and invasion of LSCC. As shown in Fig. 4A, level of p-FAK in TU686/si-ROCK1 and TU212/si-ROCK1 cells was lower than in TU686/si-nc and TU212/si-nc cells, level of FAK was not altered. On the contrary, level of p-FAK in TU686/ROCK1 and TU212/ROCK1 cells was higher than in TU686/vector and TU212/vector cells, level of FAK was not altered (Fig. 4B). To better illustrate the important role of FAK in the tumorigenesis and progression of LSCC induced by ROCK1. A FAK inhibitor (TAE226, 2.1 uM/ml) [14], which dissolved in Dimethyl Sulfoxide (DMSO) was used to treat LSCC cells. Level of p-FAK in TU686/ROCK1/TAE226 and TU212/ROCK1/TAE226 cells was lower than in TU686/ROCK1/parental, TU686/ROCK1/DMSO, TU212/ROCK1/parental, TU212/ROCK1/DMSO cells, and level of ROCK1, FAK was not altered (Fig. 4C). Transwell assays were performed to further identify the role of FAK on the tumorigenesis and progression of LSCC cells induced by ROCK1. Results indicated more TU686/ROCK1/parental ( $63 \pm 5.57$ ), TU686/ROCK1/DMSO ( $60 \pm 6.66$ ), TU212/ROCK1/parental ( $53 \pm 5.03$ ), TU212/ROCK1/DMSO cells ( $54 \pm 7.51$ ), migrated through transwell chambers compared with TU686/ROCK1/TAE226 ( $33 \pm 3.51$ ) and TU212/ROCK1/TAE226 cells ( $31 \pm 3.21$ ). Finally, invasion assays showed that TU686/ROCK1/parental ( $14 \pm 2.65$ ), TU686/ROCK1/DMSO ( $15 \pm 3.06$ ), TU212/ROCK1/parental ( $14 \pm 1.53$ ), TU212/ROCK1/DMSO cells ( $15 \pm 3.06$ ) moved through matrigel more frequently than TU686/ROCK1/TAE226 ( $7 \pm 2.89$ ) and

TU212/ROCK1/TAE226 cells ( $6 \pm 2.0$ , \*\*P < 0.01, Fig. 4D-G). All results suggested that the FAK signalling pathway may be involved in tumor-promotion effects induced by ROCK1 of LSCC.

### 5. Blocking ROCK1 impairs the metastasis of LSCC in nude mice

In order to probe the role of ROCK1 in the tumorigenesis and progression of LSCC, TU686/si-ROCK1, TU212/si-ROCK1, TU686/si-nc and TU212/si-nc, TU686/ROCK1, TU212/ROCK1, TU686/vector and TU212/vector cells were inoculated into nude mice by tail vain injection. Six weeks after inoculation, TU686/si-nc ( $3 \pm 1.00$ ) and TU212/si-nc cells ( $3.3 \pm 1.53$ ) with higher ROCK1 expression demonstrated larger and more frequent lung metastases as compared to TU686/si-ROCK1 ( $0.7 \pm 0.58$ ), TU212/si-ROCK1 cells ( $0.3 \pm 0.58$ ) with lower ROCK1 expression (\*\*P < 0.01, Fig. 5A-B). In the same way, TU686/ROCK1 ( $3.3 \pm 1.53$ ), TU212/ROCK1 cells ( $2.7 \pm 0.58$ ) with higher ROCK1 expression demonstrated larger and more frequent lung metastases as compared to TU686/vector ( $1.0 \pm 1.0$ ) and TU212/vector cells ( $0.7 \pm 0.58$ ) with lower ROCK1 expression (\*\*P < 0.01, Fig. 5C-D).

## Discussion

In our study, we intend to investigate the role of ROCK1 in tumorigenesis and progression of LSCC. The data exhibit ROCK1 is highly expressed in human LSCC tissues compared to normal tissues, and high expression of ROCK1 correlates with advanced stage and poor survival prognosis for LSCC patients. Furthermore, the data disclose potential molecular mechanism by which the tumor-promoting effects induced by ROCK1 in LSCC are mediated FAK signalling pathway. Here, all findings indicate the key role of ROCK1 as an oncogenic protein and uncover a novel molecular mechanism underlying the development and progression of LSCC.

Dysfunctional ROCK1 regulation leads to genetic instability, potentially contributing to various malignant epithelial tumors, including non-small-cell lung, prostate, pancreatic, colon, esophageal cancers. Higher ROCK1 expression in NSCLC has worse survival [15]. Prostate cancer with high ROCK1 expression was markedly related to advance tumor stage, high classical and quantitative Gleason grade, positive nodal stage, positive surgical margin, and high preoperative PSA level [16]. ROCK1 activities phosphorylation at T558 to promote the metastasis of breast cancer [17]. ROCK1 stimulates the growth and metastasis of pancreatic cancer (PC) cells in vivo and in vitro and ROCK1 may therefore have potential utility as a diagnostic and treatment target in this PC [18]. Here, in our study ROCK1 is highly expressed in human LSCC tissues in comparation to normal tissues, and high expression of ROCK1 correlates with invasion range, lymph node involvement, TNM stage and poor survival prognosis for LSCC patients.

Recent researches imply that ROCK1 has an essential role in cell migration, invasion, ECM synthesis, stress-fiber assembly, mesenchymal-epithelial transition (EMT) and resistance to chemotherapy drug therapy [19–21]. Same as the previous study, ROCK1 plays a multifunctional role in affecting proliferation, migration and invasion of LSCC. And decreasing ROCK1 expression via siRNA inhibits the ability of progression, proliferation, growth, invasion and migration in vitro, as well as pulmonary

metastasis in vivo, meanwhile, increasing ROCK1 expression via plasmid transfection has the opposite experimental results. Thus, ROCK1 promoting LSCC tumorigenesis and progression indicates that ROCK1 is a potential objective in LSCC therapy.

Numerous diverse signalling pathways, including ERK1/2 [22], MAPK [23], VEGF [24], WNT [25] and FAK [26] have been reported to promote tumor tumorigenesis and progression. FAK signalling pathway is one of the most crucial ones to promote tumorigenesis and progression of various cancers [27]. In our present study, we find ROCK1 promotes LSCC tumorigenesis and progression via the FAK pathway. Knockdown ROCK1 reduces the phosphorylation of FAK and consequently decreases the ability of progression, proliferation, growth, invasion and migration in LSCC. On the contrary, upregulation ROCK1 increases the phosphorylation of FAK and aggrandizes the ability of progression, proliferation, growth, invasion and migration of LSCC. In the next experiment, TAE226, a FAK inhibitor, is applied to indicate the role in promoting LSCC tumorigenesis and progression induced by ROCK1. All results shows that ROCK1 mediates FAK and FAK induced by ROCK1 serves as an important regulator of tumorigenesis and progression of LSCC. Therefore, targeting the molecules ROCK1 and FAK may be regarded as single or combination therapies. Nonetheless, further preclinical trials and relevant researches should be carried out to examine the effect and safe of drugs.

To sum up, we demonstrate that ROCK1 promotes LSCC tumorigenesis and progression via activation of the FAK pathway. Targeting the molecules ROCK1 and FAK might serve as potential targets for clinical LSCC treatment.

## **Materials And Methods**

## **Patient samples and Ethical statement**

Laryngeal cancer tissues and matched adjacent non-cancer samples of 30 patients were collected from the Gongli Hospital (the Second Military Medical University), Ruijin Hospital (Shanghai Jiao Tong University School of Medicine) and Shanghai Ninth People's Hospital (Shanghai Jiaotong University School of Medicine) between 2019 and 2021 year. This study was approved by the Human Research Ethics Committee of Pudong Gongli Hospital approved this study.

## **Immunohistochemical (IHC)**

Laryngeal cancer tissues and matched adjacent non-cancer samples of 30 patients were first fixed in formalin and embedded in paraffin, then xylene-dewaxed and treated in citrate buffer (0.01 mol/L, pH 6.0). Rabbit anti-ROCK1 antibody (1:2000, Cell Signaling Technology) was used to stain those samples at 4°C all night. Then samples were incubated in secondary antibody for 30 min at 37°C, and we visualized samples with DAB solution and counterstained them with haematoxylin. Two senior pathologists without knowing clinical information evaluated every sample, and a third pathologist was asked to Reevaluate the disputed samples. Five typical viewpoints were selected for IHC observation under a light microscope. The percentage of positive cells was divided into 4 grades (%): grade 0 (< 10%),

grade 1 (10%-30%), grade 2 (30–50%), grade 3 (> 50%). The staining intensity score was also divided into 4 grades (intensity): grade 0 (no staining), grade 1 (weak staining), grade 2 (moderate staining) and grade 3 (strong staining). Total immunohistochemical score = positive cell score + staining intensity score. The total score was 0,1–2,3–4, and 5–6 were defined as negative (-), weak positive ( $\pm$ ), moderate positive (+), and strong positive (++) respectively.

## Cells line and cells culture

Cells (Hep2, NH8, TU686, TU212 and Hela) were preserved by the Shanghai Institutes for Biological Sciences, Chinese Academy of Sciences. Dulbecco's modified Eagle's medium (DMEM) (Gibco company, USA) with 10% Fetal Bovine Serum (FBS, Gibco) were used to culture the above cells with 37°C temperature and 5% CO<sup>2</sup>.

## Immunofluorescent (IF)

5×10<sup>4</sup> TU686 and TU212 cells with different treatments were seeded into slides (Millipore, MA, USA) and 4% paraformaldehyde (PFA) was applied to fix cells for half an hour. PBS was used to rinse the slides for 3 times, and 5% BSA was applied to block the slides for 60 min at 37 degrees Celsius and primary antibodies were used to incubate the slides at 4°C for all night. The following day, slides were rinsed with PBS for 3 times and incubated with secondary antibodies in the dark at 37 degrees Celsius for 60 min. Anti-ROCK1 (Cell Signaling Technology) and Alexa Fluor® 488 goat (Abcam, Cambridge, MA, USA) and Alexa Fluor® 555 goat anti-rabbit IgG (Abcam, Cambridge, MA, USA) were used to IF staining. DAPI was used to visualized the nuclei of cells in the dark for 5 min. Analyzing slides by fluorescent microscopy (10x).

## Transfections

3×10<sup>5</sup> TU686 and TU212 cells with different treatments were seeded into 6-well plates and incubated for all night. ROCK1 plasmid (Myc-ROCK1-Delta3 (1-727), Gene Pharma Company, Shanghai) by lipofectamine 2000 (Invitrogen) was used to transfect and transfected cells were selected via 1200 ug/ml G418. Western Blot and frozen were used to verify selected clones.

## RNA Extraction and Quantitative Real-time PCR (qRT-PCR)

Total RNA of TU686 and TU212 cells with different treatments was extracted using Trizol reagent (Invitrogen, Carlsbad, CA, USA) and then was reverse transcribed to cDNA using Prime Script Reverse Transcriptase system (Promega, Madison, WI, USA). qRT-PCR was performed to quantify ROCK1 mRNA level with the SYBR Green PCR core Reagent kit (Applied Biosystems, Foster city, CA, USA). GAPDH was used as the endogenous reference. Data were analyzed by using the comparative Ct method. Specificity of resulting PCR products was confirmed by melting curves. The primers were designed using Primer Express v 2.0 software (Applied Biosystems, Foster City, CA, USA). The primers used in this assay were: ROCK1 forward 5'-AGG AAG GCG GAC ATA TTA GTC CCT-3' and reverse 5'-AGA CGA TAG TTG GGT CCC GGC-3', β-actin forward 5'-TGA CGT GGA CAT CCG CAA AG-3' and reverse 5'-CTG GAA GGT GGA CAG CGA GG-3'.

# **Western Blot analysis**

Total protein TU686 and TU212 cells with different treatments were lysed with RIPA buffer (Pierce, Rockford, USA). And BCA Protein Assay Kit was performed to measure the concentration of protein. Proteins with an equal amount (100 µg/sample) were electrophoresed by 10% SDS-PAGE for 2 h and transferred onto 0.22um PVDF membranes (Millipore, MA, USA). Incubating membranes with primary antibodies which included anti-ROCK1 (1:2000, Cell Signaling Technology), anti-p-FAK (1:2000, Cell Signaling Technology), anti-FAK (1:2000, Cell Signaling Technology) and GAPDH (1:5000, Abcam). After membranes incubated for all night at 4 degrees Celsius. Then incubating membranes with secondary antibody (1:5000, Cell Signaling Technology) at 4 degrees Celsius for 2 h, the proteins were visualized using enhanced chemiluminescence detection system (Amersham Bioscience, Piscataway, NJ, USA).

## **Plate colony formation assay**

Seeding TU686 and TU212 cells with different treatments into 6-well plates at  $1 \times 10^3$  and  $2 \times 10^3$  cells/well. Cells were cultured in DMEM with 10% FBS for 3 weeks, washed twice with PBS and stained with crystal violet for 30 min. Cell colonies were counted in every well.

## **Apoptosis levels using Annexin V/PI staining**

TU686 and TU212 cells with different treatments were treated with celastrol (1, 2 and 4 µM) for 48 h, then cells were harvested and washed with PBS for 3 times. Then TU686 and TU212 cells with different treatments were resuspended with 1X binding buffer prior to staining with Annexin V for half an hour at 37 degrees Celsius in the dark. TU686 and TU212 cells with different treatments were then double-stained with PI for 30 min at 37 degrees Celsius in the dark. The apoptotic TU686 and TU212 cells with different treatments were quantitatively counted by a flow cytometer.

## **In Vitro cell migration and invasion assays**

$2 \times 10^5$  TU686 and TU212 cells with different treatments after for all night starvation were plated in the coated filters in 100 µl of serum-free medium. And 600µl of medium containing 10% FBS was added to the lower chamber. The insert chambers' membrane was coated by Diluted Matrigel (BD Biosciences) for measuring the cells invasion. TU686 and TU212 cells with different treatments were counted under a high-power objective (10x) in random fields. For migration assays, the upper chamber membranes were plated on top of uncoated (Matrigel-free) filters.

## **Animal experiments**

Animals were obtained from the Institute of Zoology, Chinese Academy of Sciences. Animal experiments were carried out in accordance with the Guidelines for The Care and Utilization of Experimental Animals issued by the Institute of Experimental Animal Research. The following protocols had been approved by the medical center IRB. Animal care and treatment were conducted in accordance with NIH guidelines for the Care and Utilization of Laboratory Animals. At the end of the experiment, an overdose of sodium

pentobarbital (4%, 200 mg/kg; Sigma, Shanghai, China) was performed to kill the animals by intraperitoneal injection. And lung specimens were collected from each group for further analysis.

## In vivo metastasis

A 4-week-old male immunodeficient mouse reared at the Animal Resource Facility of Shanghai Jiao Tong University School of Medicine. The animal care and experiment were carried out in accordance with the Guidelines for "The Care and Utilization of Experimental Animals" and "The Principles for the Care and Utilization of Vertebrates", and approved by the Experimental Animal Ethics Committee of Shanghai Jiao Tong University School of Medicine. Experimental animals were grouped according to the randomization formula. In the allocation process, researchers did not understand the group allocation at different stages of the experiment, the experimental progress, the results evaluation, and the data analysis. The mice were randomly divided into groups (5 in each group): TU686 and TU212 cells with different treatments were inoculated via tail vein into the mice. After 6 months, H&E staining was performed to count pulmonary metastatic nodules. The error bar represents SEM. Paraffin-embedded TUNEL and IH staining, section them at 6 µm, and stain them with H&E. Paraffin-embedded tissue sections were dewaxed and rehydrated. For IH staining, the target recovery solution was used to thermally induce epitope recovery in microwave for 6 min. At high magnification ( $\times 400$ ), the number of tumors was calculated in the field.

## Statistical analysis

Analyze data by Graph-Pad Prism 6 software and displaying by means  $\pm$  SD. Student's t test and one-way analysis of variance (ANOVA) were used to analyze the data and the significance level was set at  $P < 0.05$ .

## Declarations

### Ethics approval and consent to participate

All procedures performed in this study were in line with the ethical standards of the institution at which this study was conducted. Informed consent was individually obtained from all participants. The Research Ethics Committee of Iran University of Medical Sciences issued IR.IUMS.FMD.REC.1399.276 for this study.

Informed consent was obtained from all individual participants, parents or legally authorized representatives of participants under legal age years old at the time of sample collection with routine consent forms.

### Availability of data and materials

The analyzed data during the current study are available from the corresponding author on reasonable request.

### Competing interests

The authors declare no conflict of interests.

## Funding

This study was conducted as part of a resident thesis and was financially supported by a grant from the Department of Pathology, Iran University of Medical Sciences (IUMS) (Grant Number# 19921).

## Authors' contributions

N.S, N.E, and F.T. designed and supervised the project, rechecked and approved all parts of the manuscript and data analysis; N.E, and F.T. wrote the manuscript. M.M., E.J. and A.M. collected the paraffin embedded tissues, collected the patient data, and performed IHC experiment. A.Z.M. analyzed and interpreted the SPSS data, helped to prepare the tables. N.S. marked the most representative areas in different parts of the tumor for the construction of TMAs blocks and scored TMAs slides after IHC staining and helped to prepare the figures. All authors read and approved the final manuscript.

## References

1. Kostrzewska-Poczekaj M, Byzia E, Soloch N, Jarmuz-Szymczak M, Janiszewska J, Kowal E, Paczkowska J, Kiwerska K, Wierzbicka M, Bartochowska A, Ustaszewski A, Greczka G, Grenman R, Szyfter K, Giefing M. DIAPH2 alterations increase cellular motility and may contribute to the metastatic potential of laryngeal squamous cell carcinoma. *Carcinogenesis*. 2019; 21.
2. Spector JG, Sessions DG, Haughey BH. Delayed regional metastases, distant metastases, and second primary malignancies in squamous cell carcinomas of the larynx and hypopharynx. *Laryngoscope*. 2016;111(6):1079-1087.
3. Upendarrao Golla, Melanie A. Ehudin, Charyguly Annageldiyev, Zheng Zeng, Diwakar Bastihalli Tukaramrao, Anna Tarren, Abhijit A. Date, Irina Elcheva, Arthur Berg, Shantu Amin, Thomas P. Loughran, Jr., Mark Kester, Dhimant Desai, Sinisa Dovat, David Claxton, Arati Sharma. DJ4 Targets the Rho-Associated Protein Kinase Pathway and Attenuates Disease Progression in Preclinical Murine Models of Acute Myeloid Leukemia. *Cancers (Basel)* 2021; 13(19): 4889.
4. Lee DH, et al. Targeted disruption of ROCK1 causes insulin resistance in vivo. *J Biol Chem*. 2009;284:11776–11780.
5. Ongusaha PP, et al. Identification of ROCK1 as an upstream activator of the JIP-3 to JNK signaling axis in response to UVB damage. *Sci Signal*. 2008;1:ra14.
6. Furukawa N, et al. Role of Rho-kinase in regulation of insulin action and glucose homeostasis. *Cell Metab*. 2005;2:119–129.
7. Samuel MS, Lopez JI, McGhee EJ. Actomyosin-mediated cellular tension drives increased tissue stiffness and  $\beta$ -catenin activation to induce epidermal hyperplasia and tumor growth. *Cancer Cell*. 2011; 19 (6): 776-791.

8. Stadler S, Nguyen CH, Schachner H, Milovanovic D, Holzner S. Colon cancer cell-derived 12(S)-HETE induces the retraction of cancer-associated fibroblast via MLC2, RHO/ROCK and Ca<sup>2+</sup> signalling. *Cell Mol Life Sci.* 2017; 74 (10): 1907–1921.
9. John C Dawson, Alan Serrels, Dwayne G Stupack, David D Schlaepfer, Margaret C Frame. Targeting FAK in anti-cancer combination therapies. *Nat Rev Cancer.* 2021 May; 21(5): 313–324.
10. Marina Roy-Luzarraga, Kairbaan Hodivala-Dilke. Molecular Pathways: Endothelial Cell FAK—A Target for Cancer Treatment. *Clin Cancer Res.* 2016 Aug 1; 22(15): 3718–3724.
11. Hsiang-Hao Chuang, Yen-Yi Zhen, Yu-Chen Tsai, Cheng-Hao Chuang, Michael Hsiao, Ming-Shyan Huang, Chih-Jen Yang. FAK in Cancer: From Mechanisms to Therapeutic Strategies. *Int J Mol Sci.* 2022 Feb; 23(3): 1726.
12. Vita M Golubovskaya. Targeting FAK in human cancer: from finding to first clinical trials. *Front Biosci.* 2014 Jan 1; 19: 687–706.
13. Tao Du, Ying Qu, Jianfang Li, Hao Li, Liping Su, Quan Zhou, Min Yan, Chen Li, Zhenggang Zhu, Bingya Liu. Maternal embryonic leucine zipper kinase enhances laryngeal cancer progression via the FAK/Paxillin pathway. *Mol Cancer.* 2014; 13: 100. Published online 2014 May 4.
14. Hiroshi Moritake, Yusuke Saito, Daisuke Sawa, Naoki Sameshima, Ai Yamada, Mariko Kinoshita, Sachiko Kamimura, Takao Konomoto, Hiroyuki Nunoi. TAE226, a dual inhibitor of focal adhesion kinase and insulin-like growth factor-I receptor, is effective for Ewing sarcoma. *Cancer Med.* 2019 Dec; 8(18): 7809–7821.
15. Changpeng Hu, Huyue Zhou, Yali Liu, Jingbin Huang, Wuyi Liu, Qian Zhang, Qin Tang, Fangfang Sheng, Guobing Li, Rong Zhang. ROCK1 promotes migration and invasion of non-small-cell lung cancer cells through the PTEN/PI3K/FAK pathway. *Int J Oncol.* 2019 Oct; 55(4): 833–844.
16. Stefan Steurer, Benjamin Hager, Franziska Büscheck, Doris Höflmayer, Maria Christina Tsourlakis, Sarah Minner. Up regulation of Rho-associated coiled-coil containing kinase1 (ROCK1) is associated with genetic instability and poor prognosis in prostate cancer. *Aging (Albany NY)* 2019 Sep 30; 11(18): 7859–7879.
17. Shuya Luo, Hui Wang, Lichuan Bai, Yiwen Chen, Si Chen, Kuan Gao, Huijie Wang, Shuwei Wu, Hanbin Song, Ke Ma, Mei Liu, Fan Yao, Yue Fang, Qinghuan Xiao. Activation of TMEM16A Ca<sup>2+</sup>-activated Cl<sup>-</sup> channels by ROCK1/moesin promotes breast cancer metastasis. *J Adv Res.* 2021 Nov; 33: 253–264.
18. Jie Wang, Zhiwei He, Jian Xu, Peng Chen, Jianxin Jiang. Long noncoding RNA LINC00941 promotes pancreatic cancer progression by competitively binding miR-335-5p to regulate ROCK1-mediated LIMK1/Cofilin-1 signaling. *Cell Death Dis.* 2021 Jan; 12(1): 36.
19. Clifford J. Whatcott, Serina Ng, Michael T. Barrett, Galen Hostetter, Daniel D. Von Hoff, Haiyong Han. Inhibition of ROCK1 kinase modulates both tumor cells and stromal fibroblasts in pancreatic cancer. *PLoS One.* 2017; 12(8): e0183871.
20. Rashmi Priya, Xuan Liang, Jessica L. Teo, Kinga Duszyc, Alpha S. Yap, Guillermo A. Gomez. ROCK1 but not ROCK2 contributes to RhoA signaling and NMIIA-mediated contractility at the epithelial

- zonula adherens. *Mol Biol Cell*. 2017 Jan 1; 28(1): 12–20.
21. Wenwen Du, Haicheng Tang, Zhe Lei, Jianjie Zhu, Yuanyuan Zeng, Zeyi Liu, Jian-an Huang. miR-335-5p inhibits TGF- $\beta$ 1-induced epithelial–mesenchymal transition in non-small cell lung cancer via ROCK1. *Respir Res*. 2019; 20: 225.
22. G. Karina Parra-Mercado, Alma M. Fuentes-Gonzalez, Judith Hernandez-Aranda, Monica Diaz-Coranguez, Frank M. Dautzenberg, Kevin J. Catt, Richard L. Hauger, J. Alberto Olivares-Reyes. CRF1 Receptor Signaling via the ERK1/2-MAP and Akt Kinase Cascades: Roles of Src, EGF Receptor, and PI3-Kinase Mechanisms. *Front Endocrinol (Lausanne)* 2019; 10: 869.
23. Yan-Jun Guo, Wei-Wei Pan, Sheng-Bing Liu, Zhong-Fei Shen, Ying Xu, Ling-Ling Hu. ERK/MAPK signalling pathway and tumorigenesis. *Exp Ther Med*. 2020 Mar; 19(3): 1997–2007.
24. Guihong Liu, Tao Chen, Zhenyu Ding, Yang Wang, Yuquan Wei, Xiawei Wei. Inhibition of FGF-FGFR and VEGF-VEGFR signalling in cancer treatment. *Cell Prolif*. 2021 Apr; 54(4): e13009.
25. Else Driehuis, Hans Clevers. WNT signalling events near the cell membrane and their pharmacological targeting for the treatment of cancer. *Br J Pharmacol*. 2017 Dec; 174(24): 4547–4563.
26. Hsiang-Hao Chuang, Yen-Yi Zhen, Yu-Chen Tsai, Cheng-Hao Chuang, Michael Hsiao, Ming-Shyan Huang, Chih-Jen Yang. FAK in Cancer: From Mechanisms to Therapeutic Strategies. *Int J Mol Sci*. 2022 Feb; 23(3): 1726.
27. Nishant P. Visavadiya, Matthew P. Keasey, Vladislav Razskazovskiy, Kalpita Banerjee, Cuihong Jia, Chiharu Lovins, Gary L. Wright, Theo Hagg. Erratum to: Integrin-FAK signaling rapidly and potently promotes mitochondrial function through STAT3. *Cell Commun Signal*. 2017; 15: 11.

## Figures

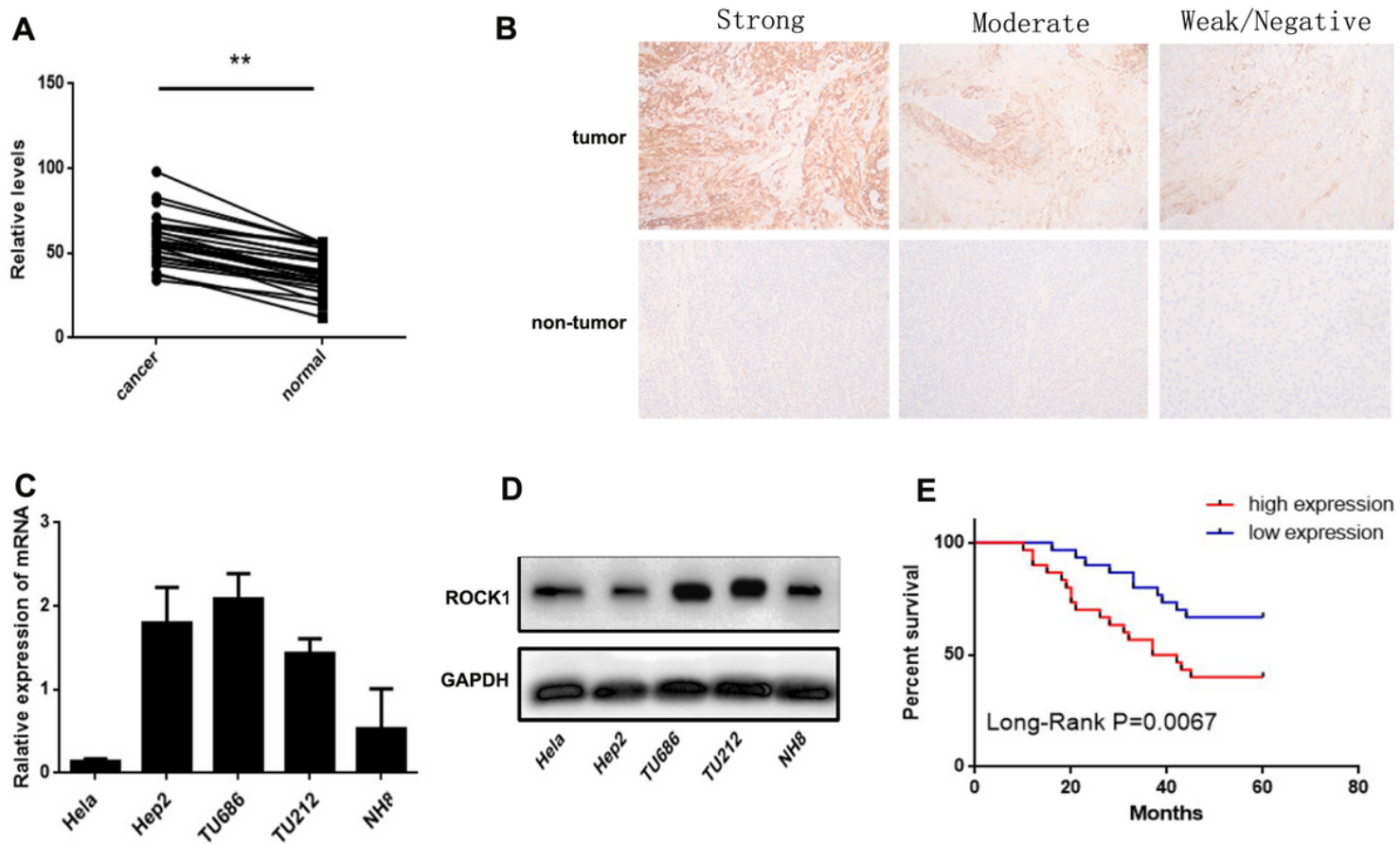


**Figure 1**

**ROCK1 overexpression in human LSCC.** **A.** Expression of ROCK1 mRNA in 30 pairs of LSCC tissues and adjacent non-tumor laryngeal tissues was quantified by qRT-PCR. Data are shown as  $2^{-\Delta Ct}$  (\*\*P < 0.01). **B.** Immunohistochemical staining of ROCK1 in LSCC tissues (magnification:  $\times 100$ ). **C.** ROCK1 mRNA expression level in the LSCC cell lines was quantified by qRT-PCR. **D.** ROCK1 protein expression level in human LSCC cell lines was examined by Western Blot. **E.** Patients with ROCK1 weak staining had a significantly benign prognosis than those with strong staining, P=0.0067.

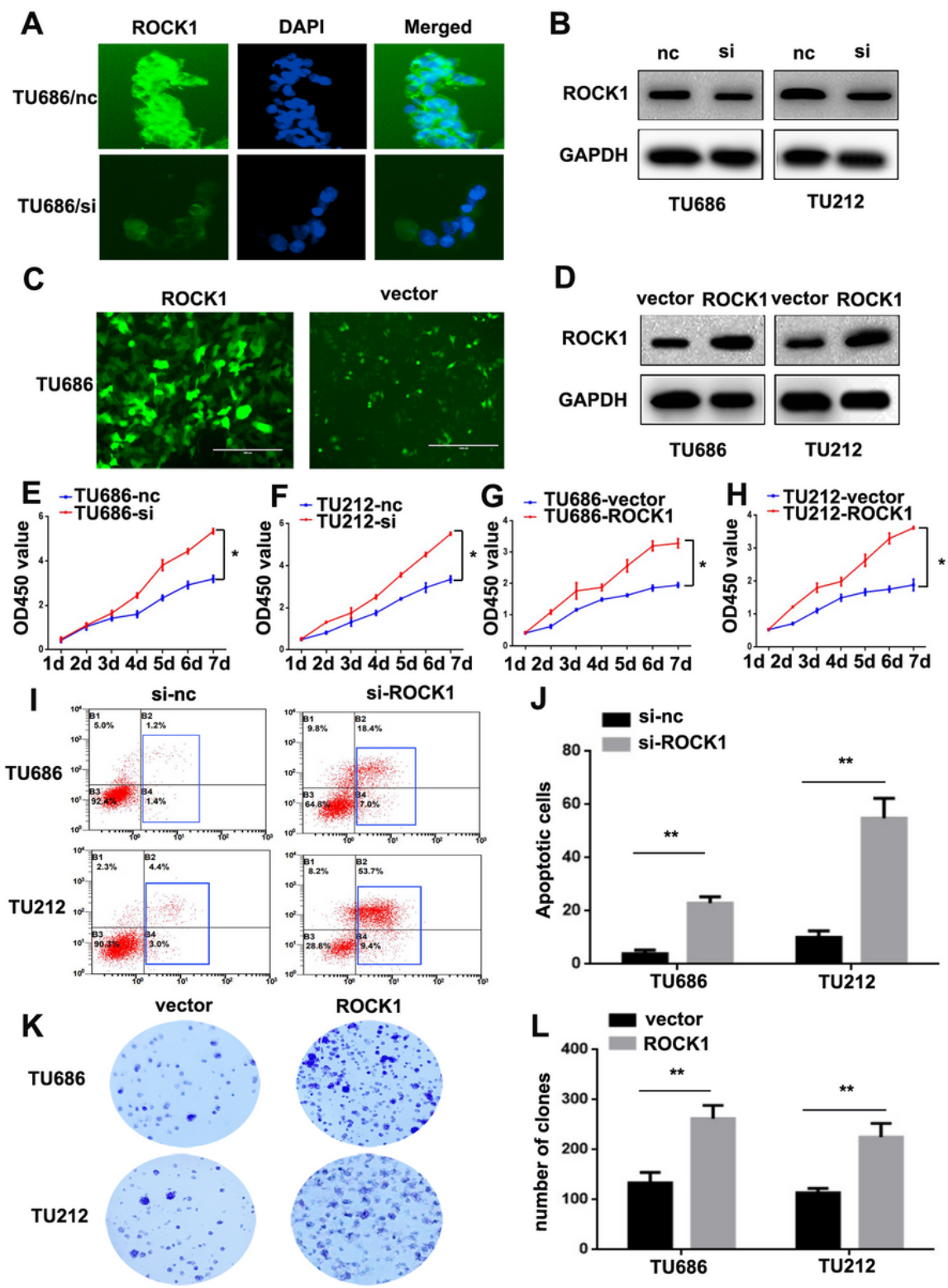


**Figure 2**

**ROCK1 promotes LSCC cells growth.** **A.** ROCK1 IF staining in TU686/si-ROCK1 and TU686/si-nc cells. ROCK1 level was reduced in TU686/si-ROCK1 cells. **B.** The inhibition effect was verified by Western Blot. ROCK1 was significantly decreased in TU686/si-ROCK1 and TU212/si-ROCK1 cells. **C.** Plasmid transfection was used to up-regulate ROCK1 in TU686 and TU212 cells, the effect of transfection was showed via IF. **D.** The expression of ROCK1 was verified by Western Blot. ROCK1 was significantly

increased in TU686/ROCK1 and TU212/ROCK1 cells. **E.F.** Knockdown of ROCK1 showed reduced cell proliferation ( $*P<0.05$ ). **G.H.** Upregulation of ROCK1 increased cell proliferation ( $*P<0.05$ ). **I.J.** Knockdown of ROCK1 induced the apoptosis of TU686 and TU212 cells ( $**P<0.01$ ). **K.L.** Upregulation of ROCK1 promoted the clone formation of TU686 and TU212 cells ( $**P<0.01$ ).

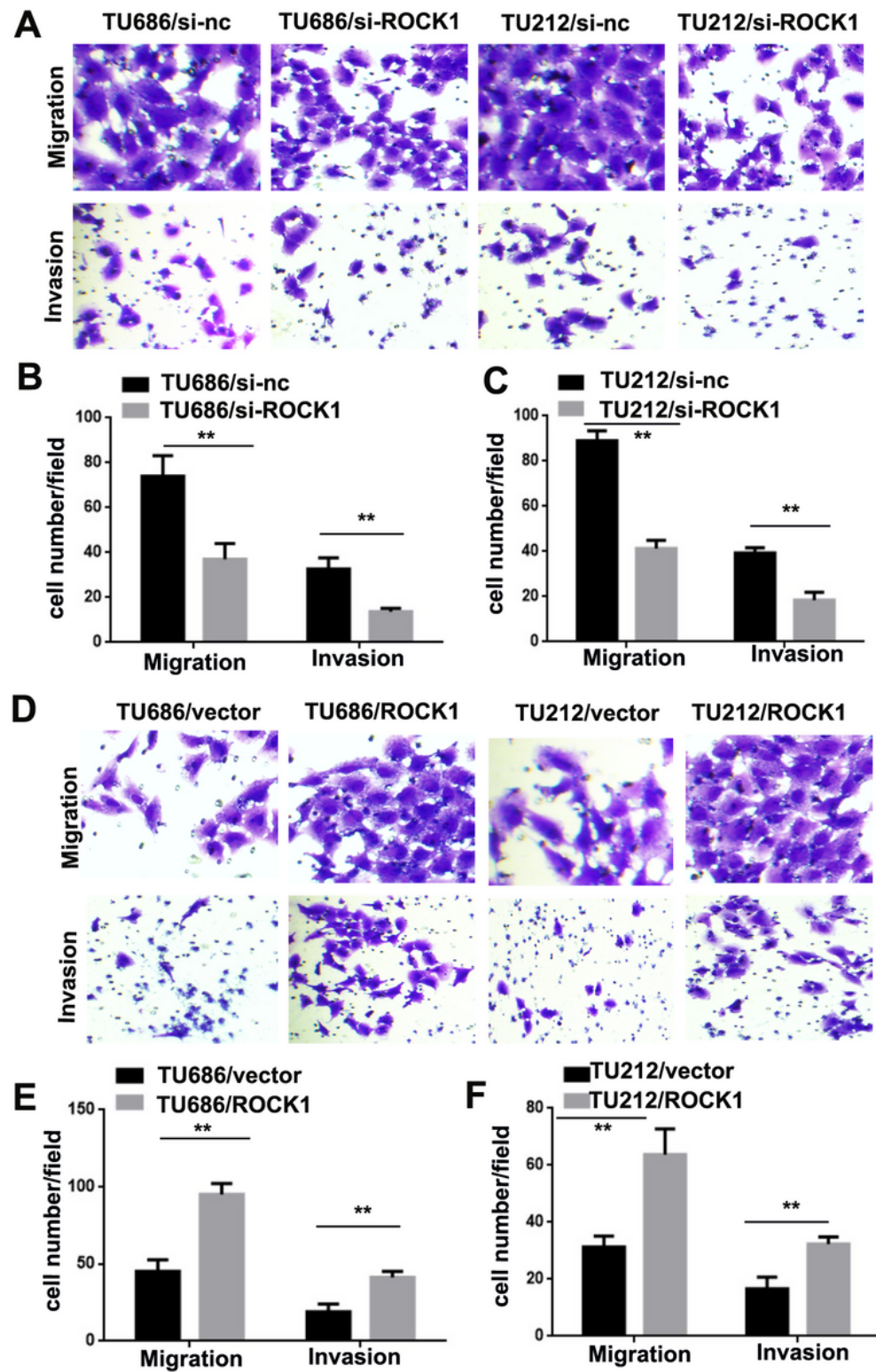
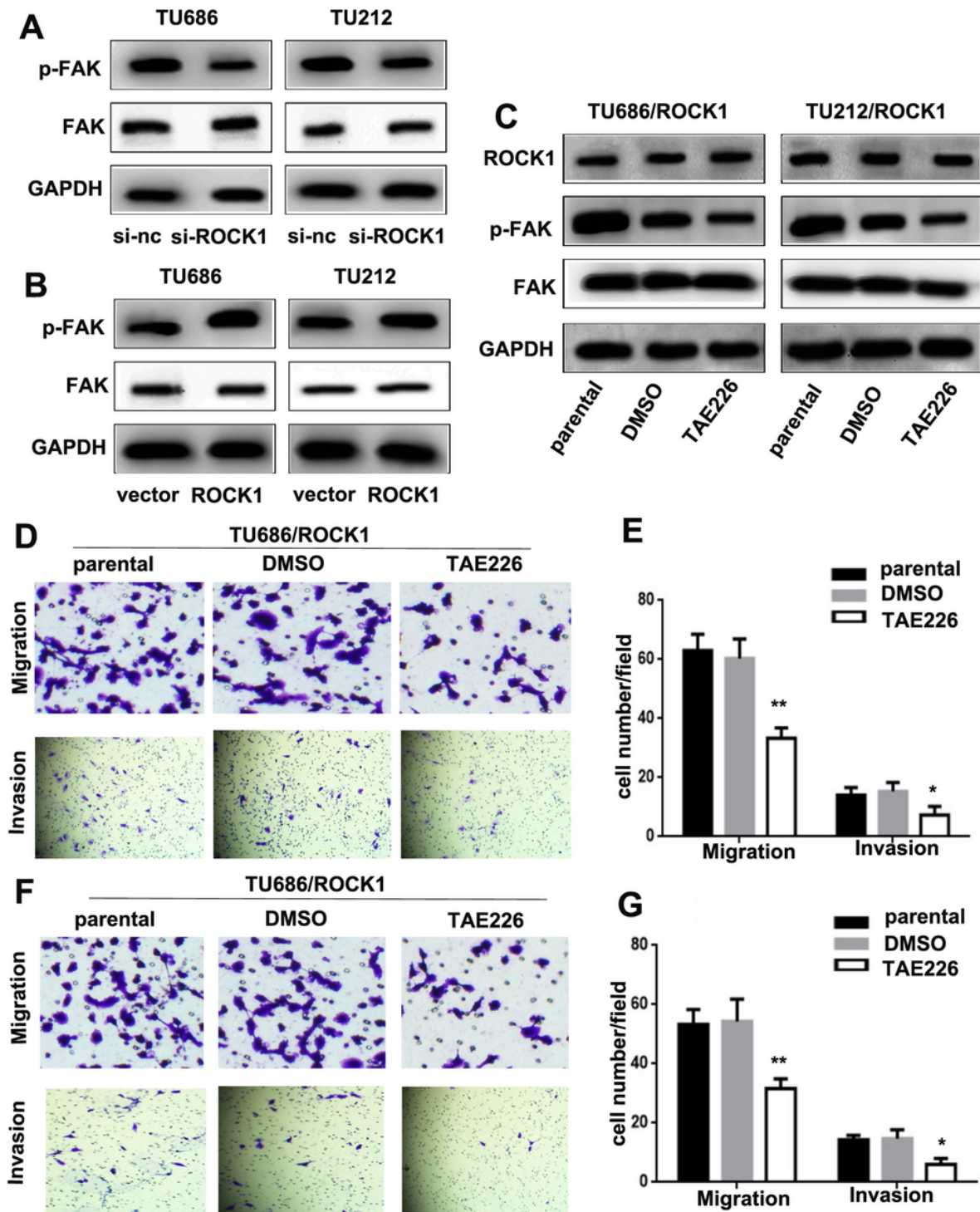


Figure 3

**ROCK1 promotes the migration and invasion of LSCC cells. A.B.C Knockdown of ROCK1 reduced the migration and invasion of TU686 and TU212 cells (\*\*P<0.01). D.E.F Upregulation of ROCK1 induced the migration and invasion of TU686 and TU212 cells (\*\*P<0.01).**



**Figure 4**

**ROCK1 promotes LSCC tumorigenesis and progression via the FAK pathway.** **A.** The expressions of p-FAK and FAK in TU686/si-ROCK1, TU212/si-ROCK1, TU686/si-nc and TU212/si-nc cells were determined by Western Blot analysis. **B.** The expressions of p-FAK and FAK in TU686/ROCK1, TU212/ROCK1, TU686/vector and TU212/vector cells were determined by Western Blot analysis. **C.** The expressions of ROCK1, p-FAK and FAK in TU686/ROCK1/parental, TU686/ROCK1/DMSO, TU212/ROCK1/parental, TU212/ROCK1/DMSO, TU686/ROCK1/TAE226 and TU212/ROCK1/TAE226 cells were determined by Western Blot analysis. **D.E.F.G.** Knockdown of FAK reduced the migration and invasion of TU686/ROCK1/TAE226 and TU212/ROCK1/TAE226 cells (\*P<0.05, \*\*P<0.01).

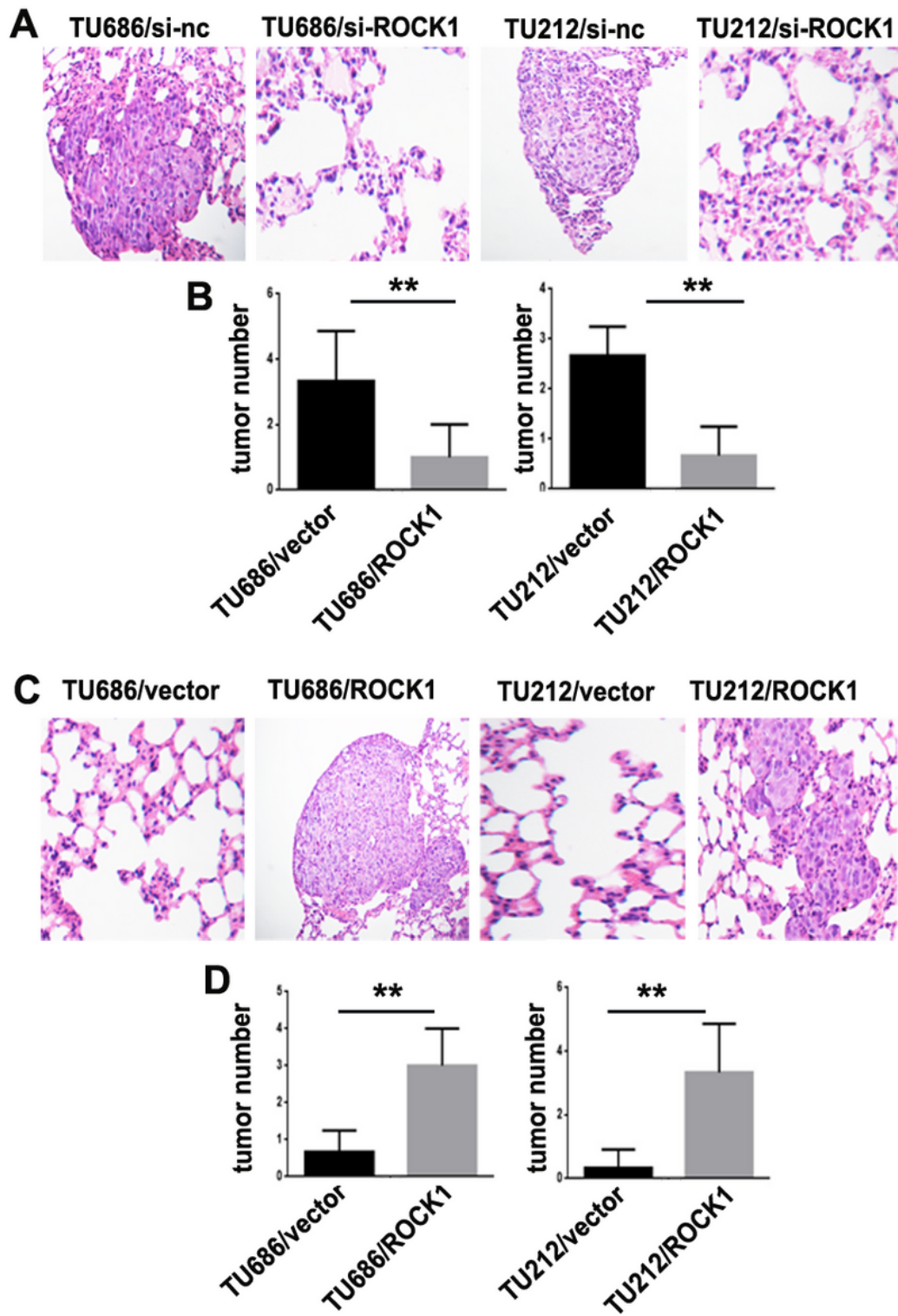


**Figure 5**

**ROCK1 induces the metastasis of LSCC in nude mice.** **A.** TU686/si-ROCK1, TU212/si-ROCK1, TU686/si-nc and TU212/si-nc cells were inoculated into nude mice and pulmonary nodules were observed after 42 days (N=5/group). H&E stains of pulmonary nodules (100×). **B.** Pulmonary tissue and nodules were quantified by H&E staining from TU686/si-ROCK1, TU212/si-ROCK1, TU686/si-nc and TU212/si-nc cells (\*\*P<0.01). **C.** TU686/ROCK1, TU212/ROCK1, TU686/vector and TU212/vector cells were inoculated into

nude mice and pulmonary nodules were observed after 42 days (N=5/group). H&E stains of pulmonary nodules (100×). **D.** Pulmonary tissue and nodules were quantified by H&E staining from TU686/ROCK1, TU212/ROCK1, TU686/vector and TU212/vector cells (\*\*P<0.01).